Relaxation Dynamics of Bidisperse Temporary Networks†

Ulf Seidel and Reimund Stadler*

Institut für Organische Chemie, Johannes Gutenberg-Universität Mainz, Becherweg 18–20, 55099 Mainz, Germany

Gerald G. Fuller

Department of Chemical Engineering, Stanford University, Stanford, California 94305-5025

Received November 19, 1993®

ABSTRACT: Simultaneous measurement of infrared dichroism and birefringence is used to examine the component relaxation in bidisperse, fully entangled melts of polybutadienes with 1% of the repeating units modified with 4-phenyl-1,2,4-triazoline-3,5-dione (urazole) groups. Since the urazole groups are capable of forming interchain hydrogen bonds, the rheological properties of these materials differ significantly from those of the analogous polybutadiene melts without polar stickers. Samples with 30, 50, and 70% long chains are examined by step strain and oscillatory shear experiments. In addition, the step strain experiments are carried out at two temperatures. All samples show a higher orientational coupling coefficient (ϵ = 0.6–0.72) than corresponding polybutadiene melts (ϵ = 0.47). The fact that orientational coupling depends on temperature and sample composition indicates that the relaxation of the chain containing stickers is strongly coupled. This feature is not incorporated in the current theory describing the relaxation of the chain containing stickers.[8]

1. Introduction

Macromolecular systems with reversible cross-links cover a broad class of materials ranging from ionomers, where ionic dipoles form aggregates[1] in the polymeric matrix, to biological macromolecules with associations induced by hydrogen bonding.[2] Polybutadiene chains with 4-phenyl-1,2,4-triazoline-3,5-dione (urazole) side groups have been established previously[3–7] as a model system showing specific interchain hydrogen bond interactions. In the most basic case, each urazole group is capable of forming two hydrogen bonds with another urazole group (Figure 1). A schematic picture of such a modified polybutadiene chain in a matrix of surrounding chains is shown in Figure 2.

The relaxation dynamics of temporary networks formed from such chains are of fundamental interest. For the monodisperse case, the "sticky reptation" theory by Leibler, Rubinstein, and Colby[8] has been demonstrated to explain the results obtained from dynamic mechanical analysis quantitatively with respect to the increase in the terminal relaxation time as compared to the corresponding chain without stickers. However, this theory is based upon a pure reptation approach that additionally accounts for specific interactions arising from the hydrogen bonds. The relaxation spectra calculated for stickered chains from this theory are almost identical in shape to those of chains without stickers but shifted to longer times. Thus, introduction of the polar stickers into PB melts should solely result in a rescaling of the relaxation time spectrum. On the other hand, the results from dynamic mechanical analysis by de Lucca Freitas et al.[3] show a significant broadening in the terminal spectrum in addition to the shift to lower frequencies. Therefore, a goal of this study was to further examine to what extent the simple rescaling of the terminal relaxation can account for the real behavior of chains carrying polar stickers. A crucial test for the theory is the examination of the relaxation behavior of bidisperse, stickered PB melts. Separate independent relaxation processes of both chain species would be expected assuming the sticky reptation model is valid. Studies of the chain dynamics[9] in binary polymer melts have shown that in the case of bidisperse systems the effects of constraint release[10–13] and orientational coupling[14–16] have to be taken into account. In the case of chains with stickers, the coupling of the chains of different length via the functional groups might alter the shape of the relaxation spectrum as well as the degree of orientational coupling.

To investigate the relaxation of chains with stickers, we chose a rheooptical technique that simultaneously allows

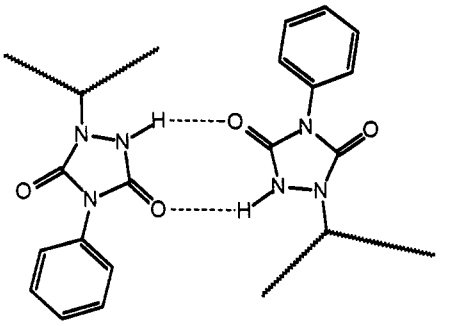

Figure 1. Formation of hydrogen bonds between urazole units.

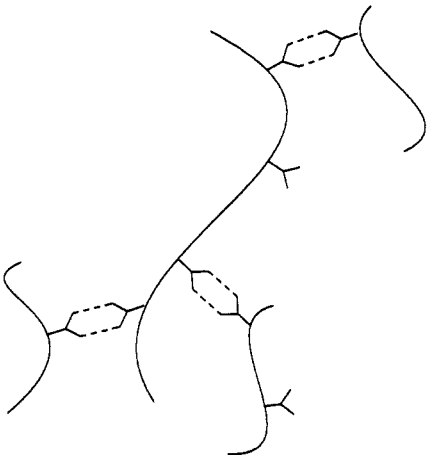

Figure 2. Schematic representation of a modified PB chain in the bulk.

† This paper is dedicated to the memory of Dale S. Pearson, a friend and colleague whose research has greatly influenced this collaboration.

® Abstract published in *Advance ACS Abstracts*, March 1, 1994.

0024-9297/94/2227-2066$04.50/0

Table 1. Characterization of the Unmodified Blend Components

polymer	M_w (GPC)	M_w/M_n (GPC)	microstructure 1,4-units (%) (^{1}H-NMR)	% of CH_2 groups deuterated
PB28	28 000	1.05	90	0
dPB29	29 000	1.05	92	70
PB109	109 000	1.09	93	0

the measurement of the bulk relaxation of the sample as well as the relaxation of a single component in bidisperse melts. Selectivity is possible by optically labeling one component in the blend by replacing a portion of the hydrogen atoms of the polymer backbone with deuterium and then performing measurements at the infrared wavelength corresponding to the carbon–deuterium stretching vibrational absorption.[17] In this way the birefringence signal ($\Delta n'$) provides a means of determining the bulk relaxation, while the dichroism signal ($\Delta n''$) due to IR absorption responds solely to the relaxation of the labeled component. Since in this study the shorter component is labeled, the orientational coupling effect (i.e., residual segmental orientation of the short chains after complete mechanical relaxation) was of special interest. Orientational coupling is an effect that has been proven present in fully compatible bidisperse melts, e.g., bidisperse PB blends.[18,19]

2. Materials and Methods

A detailed description of the apparatus, signal processing, and data acquisition is given elsewhere.[17-21]

2.1. Samples. The polybutadienes (PB) used in these experiments were prepared by anionic polymerization in cyclohexane at room temperature using *sec*-butyllithium as the initiator. After 48 h of reaction time, the living polymer chains were terminated in a degassed solvent mixture of THF/ethanol (10:1) containing 1 mL of acetic acid. Prior to further use or polar functionalization, the polymers were precipitated in 2-propanol, dissolved in THF, and reprecipitated in 2-propanol. 2,6-Di-*tert*-butyl-4-methylphenol (<0.1 wt %) was added as stabilizer. The polymers were characterized by ^{1}H-NMR and GPC (calibrated for PB by light scattering). The characterization of the polymers is summarized in Table 1.

4-Phenyl-1,2,4-triazoline-3,5-dione (PTD) was synthesized according to the literature[22] using trichloromethyl chloroformate as the in situ phosgene source. The modification of the polymers was carried out by adding the appropriate amount of PTD (standard solution in absolute ethyl acetate) to the 1 wt % solution of the PB in order to functionalize 1% of the double bonds per chain with 4-phenyl-1,2,4-triazolidine-3,5-dione (phenylurazole, PU) groups. Thus, the resulting functionalized polymers are referred to as PB109–PU1, PB28–PU1, and dPB29–PU1, respectively.

The reaction mixture was stirred overnight to ensure complete reaction. After addition of <0.1 wt % stabilizer, the modified polymer was precipitated in 2-propanol (cooled in acetone/dry ice bath) and dried under vacuum. For the preparation of the bidisperse mixtures, standard solutions, which were filtered prior to mixing, of the components (in Spectrograde THF) were prepared. With this procedure, the error in the sample component composition can be assumed to be <1%. Sample composition details are given in Table 2.

2.2. Experimental Procedure. The optical experiments on the bidisperse temporary network blends and bidisperse polybutadiene blends were performed using the same technique and setup described in previous publications.[17-21] Step strain relaxation experiments were conducted on all samples at −20 and −2 °C for the PB109–PU1/PB28–PU1 blends. Furthermore, oscillatory shear experiments on these samples and step strain experiments on the nonfunctionalized polybutadienes were carried out at −2 °C. The cooling of the flow cell was achieved through a circulation bath. The sample temperature was determined from a calibration relating the bath temperature to the sample temperature. Thus, the temperature error in the experiments is assumed to be <1 °C.

Table 2. Component Composition of the Examined Samples

sample	components (wt %)
PB109–PU1/PB28–PU1	
100/0	100% PB109–PU1
70/30	70% PB109–PU1, 10% PB28–PU1, 20% dPB29–PU1
50/50	50% PB109–PU1, 30% PB28–PU1, 20% dPB29–PU1
30/70	30% PB109–PU1, 50% PB28–PU1, 20% dPB29–PU1
0/100	80% PB28–PU1, 20% dPB29–PU1
PB109–PU1/PB28 50/50	50% PB109–PU1, 30% PB28, 20% dPB29
PB109/PB28	
100/0	100% PB109
70/30	70% PB109, 10% PB28, 20% dPB29
50/50	50% PB109, 30% PB28, 20% dPB29
30/70	30% PB109, 50% PB28, 20% dPB29
0/100	80% PB28, 20% dPB29

Table 3. τ_d Determined from Crossover of Optical Analogues of G' and G'' for −2 °C and from Complete Decay of the Birefringence Signal for −20 °C

polymer	τ_d at −2 °C (s)	τ_d at −20 °C (s)
PB28/dPB29	0.002	0.05
PB109	3	70
PB28–PU1/dPB29–PU1	0.1	2–3
PB109–PU1	50	≥500

Reproducibility of all experiments was ensured by performing at least four independent experiments with at least two different samples in oscillatory shear and at least six independent experiments with at least two different samples in step strain. A sample thickness of 0.022–0.023 cm was chosen and strain rates of 45–60% were applied. Comparison of results obtained at different strain ratios confirmed that the experiments were conducted in the linear viscoelastic regime.

For the step strain experiments, signals were averaged over at least ten steps. Data were collected for 10 s in the case of the PB109–PU1/PB28–PU1 blends and for 1 s in the cases of the PB109–PU1/PB28 blend and the pure polybutadiene blends. These time spans were chosen to ensure that enough data points were taken in the early stages of the experiments where both components of the blends contribute to the stress of the sample as well as in the late stages where only the slower relaxing component contributes to the sample stress (see relaxation times of pure components, Table 3).

Following data collection, a minimum delay, comparable to the relaxation time of the slower relaxing blend component, was chosen to ensure the complete relaxation of the sample. The data are shifted to a reference baseline to eliminate artifacts arising from detector background shifts. For the determination of the coupling coefficient (ϵ), both the birefringence ($\Delta n'$) and dichroism ($\Delta n''$) signals are normalized using a reference point at 20 ms, which is the first reliable data point after completion of the strain step. ϵ is then obtained from the final slope of the graph in a plot of the normalized dichroism versus normalized birefringence[17,19] (see Figure 3).

For the oscillatory shear experiments each data point is the average of 20 cycles at frequencies greater than 0.5 rad/s and of 5 cycles at frequencies less than 0.5 rad/s, respectively. The frequency range of 100–0.01 rad/s reflects the accessible range for this experimental setup. The raw data for the in-phase component (ψ') and the out-of-phase component (ψ'') of the birefringence and dichroism were computed. These observables are optical analogs of the storage and loss moduli ($G'_{Bi}(\omega)$, $G'_{Di}(\omega)$, $G''_{Bi}(\omega)$, and $G''_{Di}(\omega)$), using the constitutive relationships[23]

$$-\omega^2\psi'(\omega) = G'(\omega) - {}^1/_2G'(2\omega)$$

$$-\omega^2\psi''(\omega) = G''(\omega) - {}^1/_2G''(2\omega)$$

Nevertheless, the analogies to the mechanical moduli can only

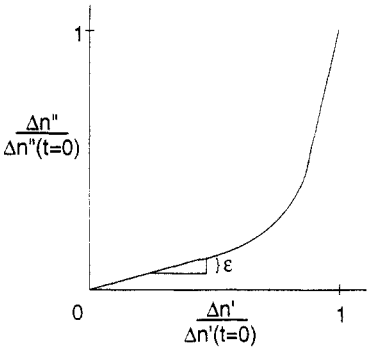

Figure 3. Graphical determination of the coupling coefficient, ϵ, from normalized dichroism and birefringence.

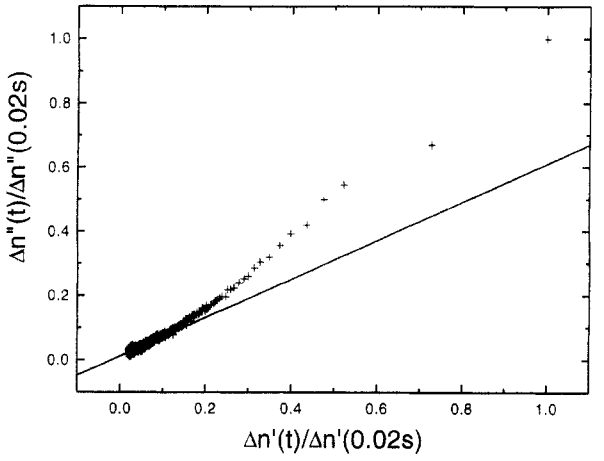

Figure 4. Determination of ϵ for PB109–PU1/PB28–PU1 30/70 at −2 °C (straight line represents the linear regression of the data points taken at long times in order to obtain ϵ).

be seen with respect to bond orientation, not necessarily with respect to chain orientation. The distinction in this work is especially important in the case of the moduli computed from dichroism. Due to orientational coupling, residual dichroism signals can still be detected at long time scales when the stress imposed on the short chains has already been dissipated.

3. Results

3.1. Step Strain Experiments. 3.1.1. PB109/PB28 Blends. For the blends of nonfunctionalized PB a coupling coefficient of $\epsilon = 0.47 \pm 0.07$, which is independent of sample composition, was found using the graphical method described above. Therefore, the results of Ylitalo et al.[24] obtained by the same experimental technique but using a different evaluation procedure have been confirmed. The method of determining ϵ in this paper has the advantage that no PB/dPB copolymer is needed for calibration, but on the other hand the relaxation times of both components have to be in the time span that is directly detectable by the experiment (>20 ms). Therefore, the experiments for the PB109/PB28 blends could only be carried out at −20 °C, the lowest temperature accessible with the setup used.

3.1.2. PB109–PU1/PB28–PU1 Blends. For the functionalized PB109–PU1/PB28–PU1 blends it was possible to run experiments at two different temperatures: −2 and −20 °C, since their relaxation times are significantly retarded compared to the nonfunctionalized polybutadienes[3,4] (see Table 3). One typical resulting plot for the samples PB109–PU1/PB28–PU1 30/70 at −2 °C and PB109–PU1/PB28–PU1 70/30 at −20 °C is shown in Figures 4 and 5. The complete set of the resulting coupling coefficients for mixtures of different compositions is summarized in Table 4. The values recorded in the table

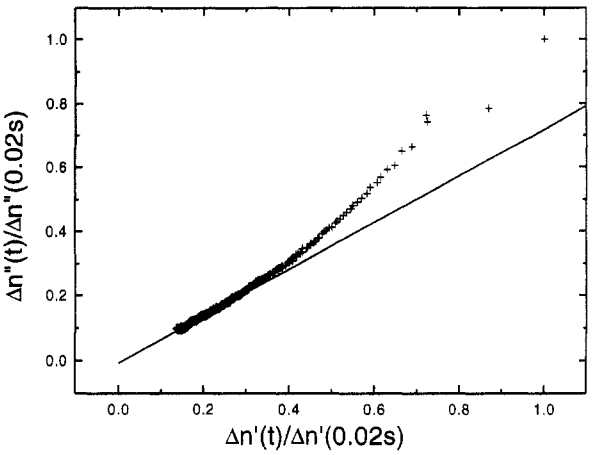

Figure 5. Determination of ϵ for PB109–PU1/PB28–PU1 70/30 at −20 °C (straight line represents the linear regression of the data points taken at long times in order to obtain ϵ).

Table 4. Orientational Coupling Coefficients from Step Strain Experiments for Different Sample Compositions and Temperatures

	coupling coefficient, ϵ	
sample	−2 °C	−20 °C
PB109–PU1/PB28–PU1		
70/30	0.70	0.72
50/50	0.66	0.70
30/70	0.60	0.64
PB109–PU1/PB28 50/50		0.01

are the mean values of at least six experiments each. The experimental errors for ϵ were found to be rather small. No deviations of more than 0.05 from the mean value reported for ϵ were found, with more than 60% of the values found for ϵ deviating only 0.02 or less from each mean value. Therefore the small differences in ϵ observed upon variation of temperature and composition reflect variations beyond the experimental uncertainty.

One important result is that all the values found for ϵ are significantly higher than for the blends of nonfunctionalized PB. Furthermore, two trends in ϵ can clearly be established. First, ϵ shows an increase with increasing fraction of long chains in the sample. This increase is not proportional to the increase of the fraction of long chains. For the increase in this fraction from the 30/70 to the 50/50 sample, ϵ increases by 0.06 for both experimental temperatures, whereas for the transition from 50/50 to 70/30 the increase is only 0.04 at −2 °C and 0.02 at −20 °C, respectively.

As a second trend ϵ also increases with decreasing temperature. The difference between the ϵ values for the two temperatures considered is 0.04 for the 30/70 and the 50/50 samples and 0.02 for the 70/30 sample.

Both of these trends observed for the PB109–PU1/PB28–PU1 blends carrying polar stickers differ from all previous results reported for polymer blends. In particular, the experiments of Ylitalo et al.[24] showed that the coupling coefficients for PB blends of long and short chains are independent of sample composition and temperature.

3.1.3. PB109–PU1/PB28 Blend. This blend, which represents a semiinterpenetrating temporary network (i.e., the long-chain matrix carries polar stickers while the shorter PB28 has no stickers), differs from the above blends since these components are not completely compatible. Although the sample looks transparent to the eye, scattering patterns indicating phase separation are detectable in a light microscope. Clear evidence for phase separation is apparent from the data shown in Figure 6. The mean

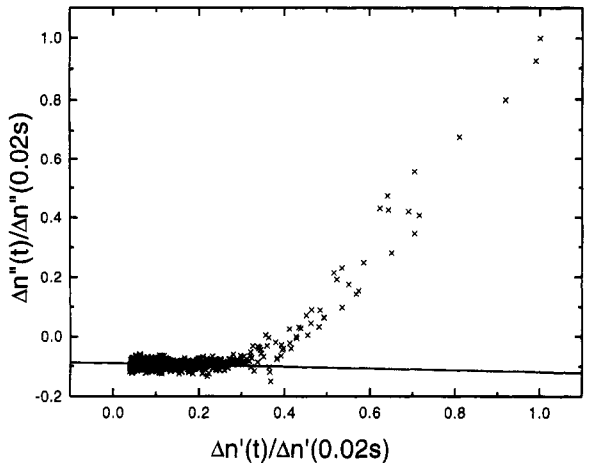

Figure 6. Determination of ϵ for PB109–PU1/PB28 50/50 at −20 °C (straight line represents the linear regression of the data points taken at long times in order to obtain ϵ).

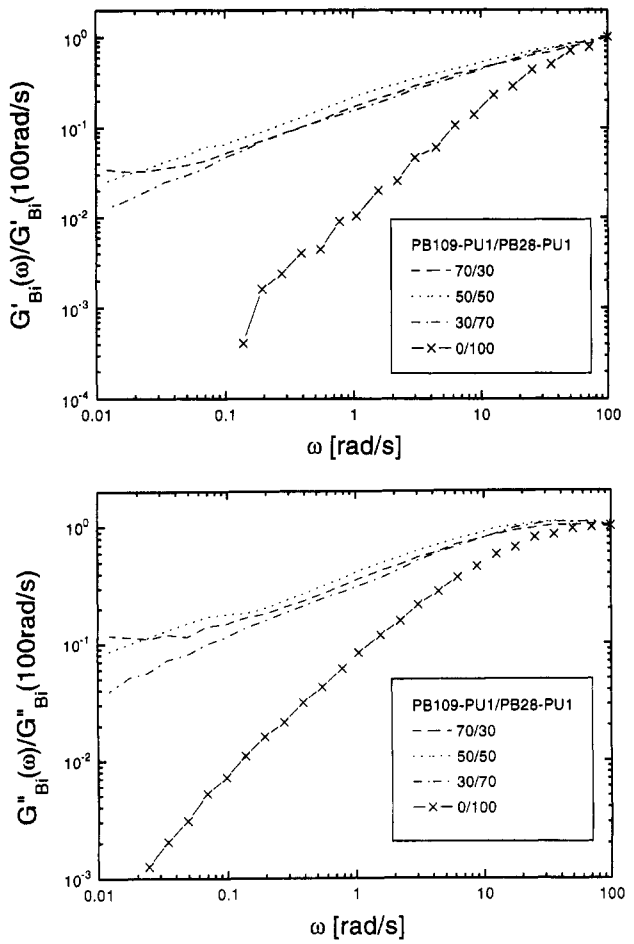

Figure 7. Optical analogs of storage moduli (a, top) and loss moduli (b, bottom) (normalized) of PB109–PU1/PB28–PU1 at −2 °C computed from birefringence.

value for ϵ obtained for this sample is 0.01, proving that there is no orientational coupling between the blend components. This reflects the fact that the individual constituents are not intimately in contact with one another but exist in separate phases.

3.2. Oscillatory Shear. 3.2.1. PB109–PU1/PB28–PU1 Blends. For the oscillatory shear experiments plots of normalized optical analogs for the storage and loss moduli ($G'_{Bi}(\omega)$, $G'_{Di}(\omega)$, $G''_{Bi}(\omega)$, and $G''_{Di}(\omega)$) are shown in Figures 7 and 8. The plots computed from birefringence (Figure 7a,b) show a broad distribution of the relaxation modes for the blends over the whole range of frequencies with a maximum in $G''_{Bi}(\omega)$ at ~100 rad/s. This maximum

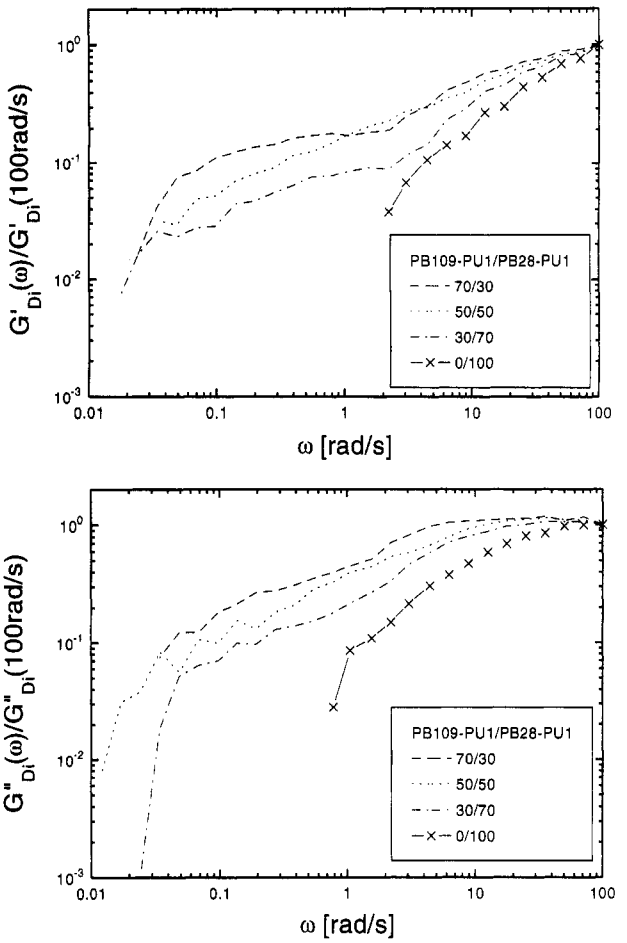

Figure 8. Optical analogs of storage moduli (a, top) and loss moduli (b, bottom) (normalized) of PB109–PU1/PB28–PU1 at −2 °C computed from dichroism.

corresponds to the maximum of the pure PB28–PU1 sample. At the very low frequency end of the plots the terminal relaxation times appear to be retarded with increasing sample content of long chains. For the dichroism, a completely different picture is obtained. In $G'_{Di}(\omega)$ (Figure 8a) two distinct plateaus can be seen. The plateau in the very high frequency range again corresponds to the plateau of the pure PB28–PU1 component. This plateau region extends to slightly lower frequencies for the blends than for the pure short component but appears to be rather similar for the different blend compositions. With decreasing frequency the optical analog of the storage modulus of the blends drops in a similar manner as $G''_{Di}(\omega)$ for the pure short chain sample. However, starting at frequencies of ~2 rad/s and extending to ~0.04 rad/s, the $G'_{Di}(\omega)$ plot for the blends exhibits a second, lower level plateau. As opposed to the high-frequency plateau, this low-frequency plateau is characterized by a modulus which is strongly dependent on the sample composition in a way that the low-frequency plateau modulus increases with increasing sample fraction of long chains.

All of the samples undergo a terminal relaxation at ~0.04 rad/s, which is rather independent of sample composition.

A very similar picture is obtained from the normalized plots of the optical analogs of loss moduli computed from dichroism $G''_{Di}(\omega)$ (Figure 8b). Here the high-frequency maximum at ~100–10 rad/s corresponds to the maximum in $G''_{Di}(\omega)$ of PB28–PU1. This maximum seems to broaden slightly with increasing amount of long chains in the blends. Going to lower frequencies, this maximum is followed by a drop in $G''_{Di}(\omega)$, similar to the behavior observed for PB28–PU1 but shifted to lower frequencies. Starting at

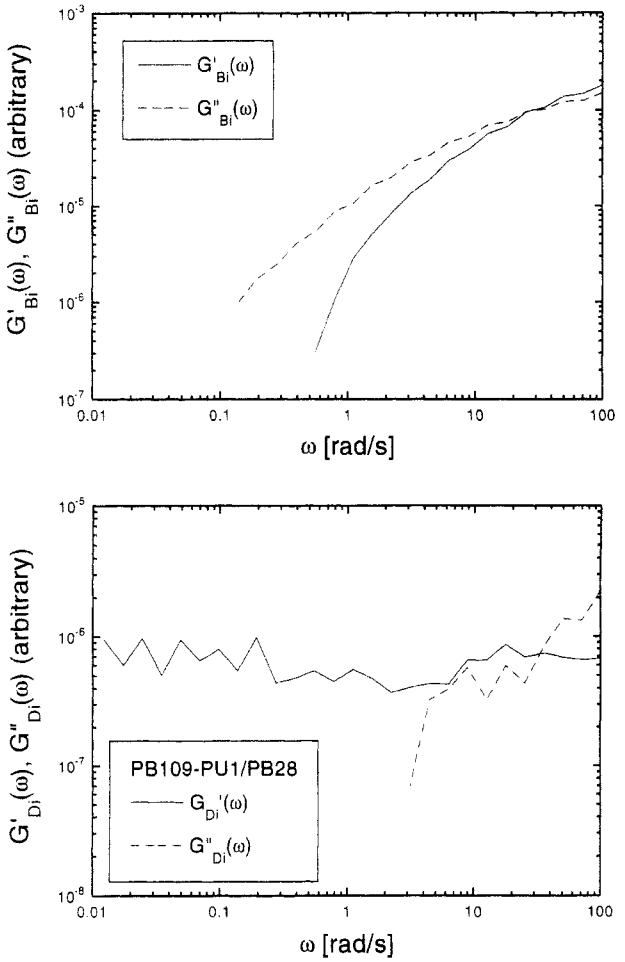

Figure 9. Optical analogs of dynamic moduli of PB109–PU1/PB28 50/50 at −2 °C computed from birefringence (a, top) and dichroism (b, bottom).

frequencies of ~2–3 rad/s, the slope of the plots for the blends again decreases to show a very broad maximum extending down to frequencies of ~0.03 rad/s. Again the loss modulus in the range of this low-frequency peak shows a strong dependence on the sample composition in the same fashion as described above for the plateau modulus.

3.2.2. PB109–PU1/PB28 Blend. For this blend the oscillatory shear experiments also reflect the occurrence of phase separation. The optical dynamic moduli plots from birefringence (Figure 9a) show relaxation behavior in between the relaxations of PB109–PU1 and PB28 but shifted strongly toward the relaxation times of PB28.

The $G'_{Di}(\omega)$ and $G''_{Di}(\omega)$ plots (Figure 9b) show a relaxation where only the very last part of the terminal relaxation regime can be detected in $G''_{Di}(\omega)$ before the signals fall below a detectable threshold. This graph is identical with the one of PB28. In addition, $G'_{Di}(\omega)$ shows a constant value over all frequencies, which may indicate contributions of form dichroism arising from the phase domains polluting the signal of the intrinsic dichroism arising from carbon–deuterium stretching absorption.

4. Discussion

The data obtained from the oscillatory shear experiments show a broad distribution of the relaxation times over the whole experimentally accessible frequency range in the optical analogs of the storage and the loss moduli computed from birefringence. This is a consequence of the broadening of the relaxation time spectrum which was already observed for monodisperse urazole-modified polybutadienes by de Lucca Freitas et al.[3,4] As a consequence, the relaxation time distribution for bidisperse melts does not show two distinct maxima in $G''_{Bi}(\omega)$ (as is the case for bidisperse polybutadiene blends[19]). Rather a decrease in $G'_{Bi}(\omega)$ and $G''_{Bi}(\omega)$ (Figure 7a,b) over the whole frequency range was observed, with a maximum appearing at 100 rad/s, indicating an even further increase in the effective polydispersity. The differences observed in the various blends at the lowest frequencies are likely to be due to constraint release effects resulting in a slightly decreasing terminal relaxation time with decreasing sample content of PB109–PU1. From optical analogs of the storage and loss moduli computed from the dichroism in-phase and out-of-phase signals, respectively, additional information with respect to the orientational coupling can be obtained. The two plateaus which can be seen in $G'_{Di}(\omega)$ (Figure 8a) (e.g., the two maxima in $G''_{Di}(\omega)$ (Figure 8b)) arise for different reasons. At high frequencies the moduli analogs of the blends show a similar behavior as in the pure sample of PB28–PU1 chains. At low frequencies, on the other hand, the blend moduli do not show the complete relaxation as observed in the sample without long PB109–PU1 chains. Instead residual bond orientation caused by orientational coupling to the still oriented long chains is observed. The dependence of this orientational coupling on blend composition is evident from parts a–c of Figure 10, which show the normalized optical analogs of the storage moduli computed from birefringence and dichroism for the different blend compositions. While the birefringence signals are very similar, except at very low frequencies due to constraint release effects as discussed above, the dichroism signals at lower frequencies show a significant decrease with the decrease in the long-chain PB109–PU1 fraction of the blend. This composition dependence has been quantitatively evaluated by the transient step strain experiments.

The confirmation of the results of Ylitalo et al.[24] of an orientational coupling coefficient of $\epsilon = 0.45$ of the short chains in bidisperse PB melts by these transient experiments validates the data evaluation procedure used to obtain the present results. In addition, it has been confirmed that ϵ does not depend on composition and temperature in the case of the bidisperse polybutadiene melts without stickers.

In contrast, the coupling coefficients listed in Table 3 strongly suggest that two contributions have to be considered for the PB109–PU1/PB28–PU1 systems. The first contribution is assumed to arise from the effect of excluded volume interaction in the anisotropic field (also referred to as nematic interaction[14]) in bidisperse homopolymer blends, thus giving rise to an orientational coupling coefficient of $\epsilon = 0.45$ for the case of 1,4-polybutadiene. This coupling coefficient (which shall be called $\epsilon_{intrinsic}$) has been proven to be independent of both sample composition and temperature.[24] In addition to the intrinsic orientational coupling, a second, superimposed interaction affecting ϵ is observed for the temporary networks discussed here. This additional effect has to be related to the hydrogen bond complexes between the urazole groups between long and short chains (and shall be called ϵ_{excess}). This assignment is strongly backed by the observation that ϵ for the samples considered here is dependent on both temperature and sample composition. Both dependencies can be readily explained:

(a) The increase of ϵ at lower temperatures results from the increase in the fraction of the hydrogen-bonded stickers and thus from the longer lifetime of urazole–urazole complexes ($\tau_{u-u\ complex} = 5 \times 10^{-5}$ s at 0 °C[8]).

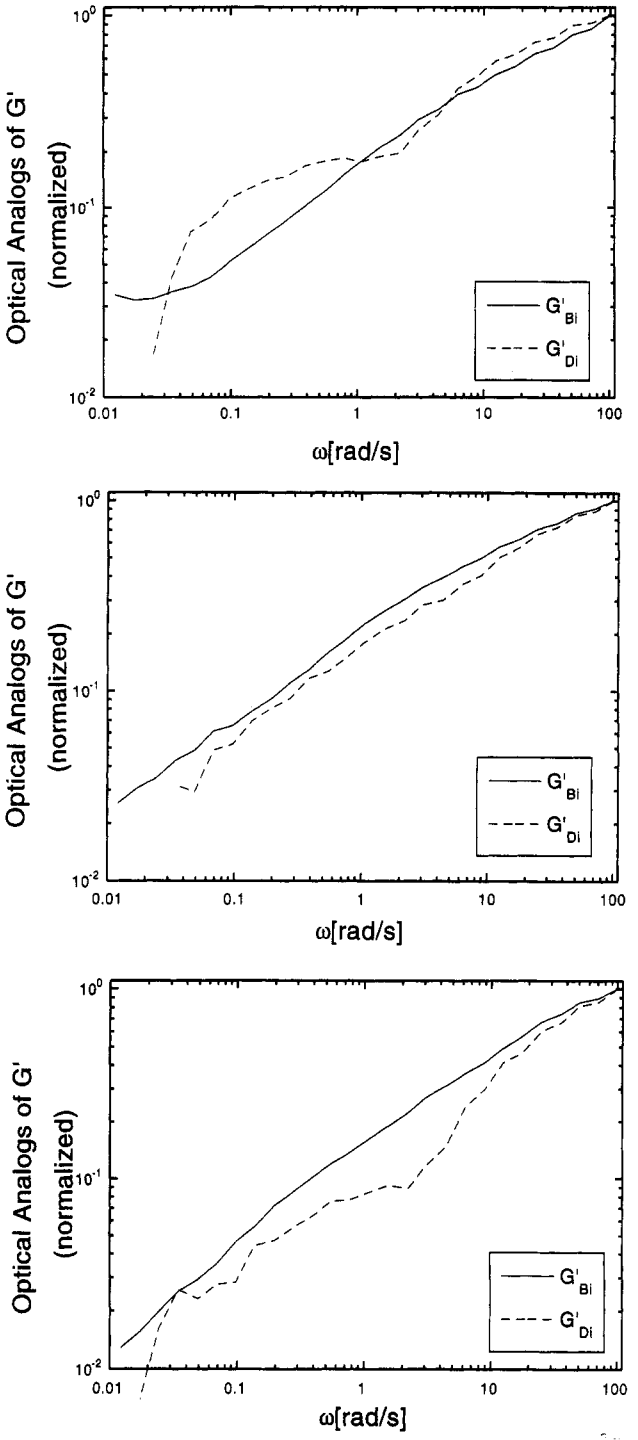

Figure 10. Optical analogs of storage moduli of PB109–PU1/PB28–PU1 70/30 (a, top), 50/50 (b, middle), and 30/70 (c, bottom) at −2 °C computed from birefringence and dichroism.

(b) The increase of ϵ with increasing fraction of long chains (e.g., PB109–PU1) corresponds to the increasing probability of urazole groups of a short PB28–PU1 chain, which has relaxed mechanically, to be bound to stickers of a PB109–PU1 chain. The basis for this explanation is the obvious assumption that a complex between two urazole groups of PB28–PU1 chains does not give rise to $\epsilon > \epsilon_{intrinsic}$ since these complexes do not retard the relaxation of these chains over their relaxation in a pure PB28–PU1 sample. Thus ϵ_{excess} is completely due to complexes between urazole groups of long PB109–PU1 chains and short PB28–PU1 chains (or, more precisely, short dPB29–PU1 chains). The number of these complexes rises with increasing fraction of PB109–PU1 chains.

Nevertheless, the increase in ϵ_{excess} (and therefore $\epsilon = \epsilon_{intrinsic} + \epsilon_{excess}$) is not proportional to the increase in the PB109–PU1 fraction. A more quantitative study of this effect will be subject to further investigation.

Another surprising result reported in this paper is the experiment of the coupling coefficient found for the PB109–PU1/PB28 blend. This blend, which is found to be phase separated, exhibits no orientational coupling at all, since the mean coupling coefficient was found to be $\epsilon = 0.01$. Evidently, the experimental procedure applied here appears to be a powerful tool for examining compatibility on a segmental level.

Conclusion and Outlook

The sticky reptation model,[8] which was found to give a satisfactory description of the terminal relaxation behavior of polymer chains containing polar stickers, obviously does not provide a satisfactory description of the relaxation properties of the bidisperse polybutadiene melts, where it predicts rather independent terminal relaxation properties of the blend components. The relaxation is smeared over a broad range of frequencies, in agreement with the experimental results on monodisperse chains with stickers, which already showed a broadening of the relaxation time spectrum.

The observed broadening may be the result of the random substitution of the polymer with functional stickers. This inherent randomness may result from substitution, where two (or maybe three) functional groups are located in neighboring (or closely neighboring) positions along the chain and form a "multiple sticker". According to a recent theoretical description by Nyrkova, Khokhlov, and Doi[25] on the formation of dipole–dipole clusters in ionomers, the stability of complexes (clusters) which results if such multiple stickers meet is largely improved. This would result in a variation of the lifetimes and efficient friction coefficients of the hydrogen bond contacts and could explain the broadening of the terminal spectrum. Recent dielectric experiments show indeed that the dynamics of complex formation shows a strong heterogeneity if the fraction of stickers is increased.[26]

One additional feature of the experiments discussed in this paper, which is not described by the theory, is related to the orientational coupling. The result that the segmental coupling between different chains is a function of sticker concentration, temperature, and binary blend composition indicates that some facets of the basic physics of interacting chains are not yet included in the theory.

Acknowledgment. The help of Jeff Zawada is gratefully acknowledged. In addition to providing the experimental setup in its present state, he supported the ongoing work with his detailed technical knowledge as well as with many helpful discussions. This work is supported by the German Science foundation (DFG) through the Gerhard Hess program for R.S. U.S. thanks the Fonds der Chemischen Industrie (FdCh) and the Graduiertenkolleg "Chemie und Physik supramolekularer Systeme" for financial support. R.S. is indebted to R. H. Colby for numerous discussions concerning the conception of the experiments presented in this paper. G.G.F. is grateful to the NSF for support of this research through Grant DMR 9120360.

References and Notes

(1) Eisenberg, A.; Baily, F. E., Eds. *Coulombic Interactions in Macromolecular Systems*; ACS Symposium Series 302; American Chemical Society: Washington, DC, 1986.
(2) Burchard, W. *Br. Polym. J.* **1985**, *17*, 154.

(3) de Lucca Freitas, L.; Stadler, R. *Macromolecules* **1987**, *20*, 2478.
(4) de Lucca Freitas, L.; Stadler, R. *Colloid Polym. Sci.* **1986**, *264*, 773.
(5) de Lucca Freitas, L.; Burgert, J.; Stadler, R. *Polym. Bull.* **1987**, *17*, 431.
(6) Stadler, R.; de Lucca Freitas, L. *Macromolecules* **1989**, *22*, 714.
(7) de Lucca Freitas, L.; Stadler, R. *Polym. Prepr. (Am. Chem. Soc., Div. Polym. Chem.)* **1989**, *30*/1, 87.
(8) Leibler, L.; Rubinstein, M.; Colby, R. H. *Macromolecules* **1991**, *24*, 4701.
(9) Doi, M.; Edwards, S. F. *The Theory of Polymer Dynamics*; Clarendon: Oxford, 1986.
(10) Graessley, W. W. *Adv. Polym. Sci.* **1982**, *42*, 67.
(11) Rubinstein, M.; Colby, R. H. *J. Chem. Phys.* **1988**, *89*, 5291.
(12) Rubinstein, M.; Helfand, E.; Pearson, D. S. *Macromolecules* **1987**, *20*, 822.
(13) des Cloizeaux, J. *Macromolecules* **1990**, *23*, 4678.
(14) Doi, M.; Pearson, D.; Kornfield, J.; Fuller, G. G. *Macromolecules* **1989**, *22*, 1488.
(15) Merrill, W. W.; Tirrell, M.; Jarry, J.-P.; Monnerie, L. *Macromolecules* **1989**, *22*, 896.
(16) Watanabe, H.; Kotaka, T.; Tirrell, M. *Macromolecules* **1991**, *24*, 201.
(17) Kornfield, J. A.; Fuller, G. G.; Pearson, D. S. *Macromolecules* **1989**, *22*, 1334.
(18) Kornfield, J. A.; Fuller, G. G.; Pearson, D. S. *Rheol. Acta* **1990**, *29*, 105.
(19) Ylitalo, C. M.; Kornfield, J. A.; Fuller, G. G.; Pearson, D. S. *Macromolecules* **1991**, *24*, 749.
(20) Zawada, J. A. Doctoral Dissertation, Stanford University, Stanford, 1993.
(21) Kornfield, J. A. Doctoral Dissertation, Stanford University, Stanford, 1988.
(22) Cookson, R. C.; Gupte, S. S.; Stevens, J. D. R.; Watts, C. T. *Org. Synth.* **1971**, *51*, 121.
(23) Kornfield, J. A.; Fuller, G. G.; Pearson, D. S. *Macromolecules* **1991**, *24*, 5429.
(24) Ylitalo, C. M.; Zawada, J. A.; Fuller, G. G.; Abetz, V.; Stadler, R. *Polymer* **1992**, *33* (14), 2949.
(25) Nyrkova, I. A.; Khokhlov, A. R.; Doi, M. *Macromolecules* **1993**, *26*, 3601.
(26) Mueller, M.; Kremer, F.; Schirle, M.; Stadler, R., unpublished.